



“Gheorghe Asachi” Technical University of Iasi, Romania



PHOTOCATALYTIC DEGRADATION OF ATRAZINE USING ZINC OXIDE TEXTURALLY MODIFIED WITH STICKY RICE STARCH TEMPLATE AND DOPED WITH TRANSITION METALS

Pummarin Khamdahsag^{1*}, Nuttaporn Pimpha², Raumporn Thongruang³, Nurak Grisdanurak^{4,5}, Mark A. Nanny⁶, Jatuporn Wittayakun^{1*}

¹ Suranaree University of Technology, School of Chemistry, Institute of Science, Nakhon Ratchasima 30000, Thailand

² National Nanotechnology Center, National Science and Technology Development Agency, Thailand Science Park, Pathumthani 12120, Thailand

³ Thammasat University, Department of Physics, Pathumthani 12121, Thailand

⁴ Thammasat University, Department of Chemical Engineering, Pathumthani 12121, Thailand

⁵ Thammasat University, Center of Excellence on Environmental Catalysis and Adsorption, Pathumthani 12121, Thailand

⁶ University of Oklahoma, School of Civil Engineering and Environmental Science, Norman, Oklahoma 73019, USA

Abstract

Atrazine is a herbicide used widely with a large quantity in Thailand and can contaminate in surface and groundwater. This work investigated atrazine removal from an aqueous solution by catalytic photodegradation using oxides of metal-cerium-zinc (M-Ce-ZnO, M = Ag, Fe, and Cu). ZnO is texturally modified with sticky rice starch template, doped with cerium (Ce) and either Ag, Fe, or Cu with the M:Ce:Zn molar ratio of 0.005:0.005:1. The catalysts were characterized by XRD, UV-Vis-DRS, and N₂ adsorption-desorption analysis; and tested in a batch reactor under visible light. 0.005Ag-0.005Ce-ZnO exhibited a higher atrazine removal than 0.005Fe-0.005Ce-ZnO and 0.005Cu-0.005Ce-ZnO. Thus, a further investigation was carried out on 0.005Ag-0.005Ce-ZnO with various atrazine concentrations. The photocatalysis was explained by Langmuir-Hinshelwood-Hougen and Watson (LHHW) kinetics. The reaction rate constant was higher than the adsorption equilibrium constant indicating that the photocatalytic reaction was a key role in the atrazine removal. In the presence of humic acid, a representative of natural organic matter, a competition with atrazine was observed. To determine the degradation pathway, several intermediates were detected by liquid chromatography-mass spectrometry including 2-isopropylamino-1,3,5-triazine which was not previously reported. The efficiency of 0.005Ag-0.005Ce-ZnO suggests a possibility for the application under the sunlight.

Key words: atrazine, metal doped ZnO, photocatalysis, sticky rice starch, textural modification

Received: December, 2013; Revised final: March, 2015; Accepted: April, 2015; Published in final edited form: November 2018

1. Introduction

Atrazine (2-chloro-4-ethylamino-6-isopropylamino-1,3,5-triazine, see structure in Fig. 1) is a herbicide which is used widely with a large quantity in Thailand to control broadleaf and grassy weeds in a variety of crops. Atrazine is one of the top

five hazardous chemicals imported to Thailand with a quantity of approximately six thousand tons in 2012 (ARO, 2012). It was used as much as 1.5-4.5 kg/hectare for overall weed control (Sukjaroen and Prayoonrat, 2001). With such amount, atrazine could contaminate either surface or groundwater and raise environmental impacts to bacteria, plankton, plants,

* Author to whom all correspondence should be addressed: e-mail: u4302273@yahoo.com, jatuporn@sut.ac.th; Phone: +66 994954297, +66 44224256; Fax: +66 44224185, +66 44224185

animals, and humans. Its distribution in a field resulted in a decrease in frog population (Hayes et al., 2003). Low concentrations of atrazine could result in ecological consequences to freshwater mussel quantities (Flynn and Spellman, 2009) and dietary exposure data suggested oncogenic risk to humans (U.S. EPA., 1988).

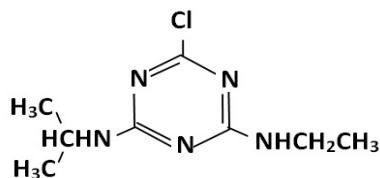


Fig. 1. Structure of atrazine

There was a report about atrazine contamination at various sites in Thailand with concentrations in the range 58-106 $\mu\text{g/L}$ (Kruawal et al., 2005). Those values are much higher than the maximum allowable concentration for drinking water (2 $\mu\text{g/L}$) and water quality for consumption and agricultural usage (3 $\mu\text{g/L}$) (WQMB, 2012).

Atrazine has a half-life longer than 6 months (U.S. EPA., 2003). It can be degraded slowly by photolysis under UV radiation which is approximately 4-5 % part of sunlight. The degradation could be enhanced in the presence of catalysts such as TiO_2 and ZnO as their band gaps are suitable for the UV absorption. The ability of ZnO and TiO_2 to degrade atrazine was in the same range (rate constant (k) $27\text{-}327 \times 10^{-3} \text{ min}^{-1}$) and higher than that of Sr-TiO_3 , ZnS , Fe_2O_3 , and FeTiO_3 ($k = 0.15\text{-}0.70 \times 10^{-3} \text{ min}^{-1}$) (Lackhoff and Niessner, 2002). The ability of ZnO to degrade atrazine under the sunlight can be enhanced doping with cerium (Ce) to enhance the absorption of visible light (Chang et al., 2014).

Recently, Khamdahsag et al. (2012) reported a preparation of Ce-ZnO using sticky rice starch and polyvinylpyrrolidone as templates to improve the distribution of Ce and Zn ions. Ce-ZnO from the starch template exhibited superior physicochemical properties and photocatalytic ability in atrazine degradation to the other. Thus, a further attempt was made in this work to improve the photocatalytic performance of Ce-ZnO by doping with Ag, Fe or Cu. Those elements were reported to give a red shift in UV-Vis absorption spectra of ZnO (Li and Haneda 2003; Li et al., 2004; Ren et al., 2010; Vidyasagar et al., 2011; Zhang et al., 2011). The ZnO doped with Ag, Fe, or Cu was an active photocatalyst to remove methylene blue (Ren et al., 2010), methyl orange (Hsu and Chang, 2014; Zhang et al., 2011), acetaldehyde (Li et al., 2004), aniline (Jafari et al., 2016), rhodamine B (Tian et al., 2010; Xin et al., 2008), and food black 2 (Hsu and Chang, 2014).

Photocatalytic degradation of atrazine has been studied by many researchers and its reaction mechanism has been proposed. Alkyl substituted groups in atrazine was not mineralized completely by photocatalytic degradation and some intermediates were detected (Minero et al., 1996; Yola et al., 2014).

Cyanuric acid or 2,4,6-trihydroxyl-1,3,5-triazine was reported to be a stable final product from photocatalytic degradation of atrazine by TiO_2 and TiO_2 nanoparticles with boron enrichment, both under UV irradiation (McMurray et al., 2006; Yola et al., 2014) and with $\text{Na}_2\text{S}_2\text{O}_8$ oxidant (Minero et al., 1996). An attempt was made in this work to identify intermediates from atrazine photodegradation on the ZnO-based catalysts under visible light to elucidate the degradation pathway.

2. Experimental

2.1. Synthesis of photocatalysts

All catalysts were prepared using sticky rice starch template with a method from the literature (Khamdahsag et al., 2012). First, sticky rice starch (Erawan Brand, Thailand) was mixed with 100 mL of water and blended under vigorous stirring at 80°C for 30 min to obtain a homogeneous gel. Then, a solution containing AgNO_3 (Carlo Erba Reagents, 99.8%), $\text{Fe}(\text{NO}_3)_3 \cdot 9\text{H}_2\text{O}$ (Merck, 99.0-101.0%), or $\text{CuSO}_4 \cdot 5\text{H}_2\text{O}$ (Carlo Erba Reagents, 98-102%); $\text{Ce}(\text{NO}_3)_3 \cdot 6\text{H}_2\text{O}$ (Acros Organics, 99.5%) and $\text{Zn}(\text{NO}_3)_2 \cdot 6\text{H}_2\text{O}$ (Acros Organics, 98%) was prepared separately in 20 mL of water and then added into the starch gel. The molar ratio M:Ce:Zn was 0.005:0.005:1 (M = Ag, Fe, Cu). The mixture was stirred at 80 °C for another 30 min and subsequently oven-dried at 100°C for approximately 48 h. The dried precursors were calcined at 550 °C for 3 h at a heating rate of 2 °C/min. Finally, the obtained material (0.005Ag-0.005Ce-ZnO, 0.005Fe-0.005Ce-ZnO, and 0.005Cu-0.005Ce-ZnO) was ground and sieved to obtain particle size < 0.150 mm. The catalyst color was light grey, orange, and grey, respectively.

2.2. Characterization

Crystal phases of 0.005Ag-0.005Ce-ZnO, 0.005Fe-0.005Ce-ZnO, and 0.005Cu-0.005Ce-ZnO were analyzed by X-ray diffraction (XRD) on a Bruker AXS Model D8 Discover with a Cu K α radiation ($\lambda = 1.5406 \text{ \AA}$). The scan range was 20-80° with an increment of 0.02°/step, and a scan speed of 0.1 sec/step. Their surface areas were determined by nitrogen adsorption on an Autosorb-1 Quantachrome instrument with the Brunauer-Emmett-Teller (BET) method. UV-Vis diffusive reflectance absorption spectra (UV-Vis-DRS) were obtained from a UV-Vis spectrophotometer (U-3501 HITACHI) in the range 300-800 nm using powder of BaSO_4 as a reference.

2.3. Reactor setup

Photocatalytic degradation of atrazine was conducted in a beaker-type batch reactor in a cooling water bath to maintain the temperature at $25 \pm 1^\circ\text{C}$ (Fig. 2). Five tungsten lamps (Philips E27 100W) were set to be perpendicular to a 1000-mL borosilicate glass beaker with a distance 5 cm. Average visible and UV

light intensity was 607.12 W/m^2 and 0.0 mW/cm^2 was measured by a solarimeter (Kimo SL100, France) and UV-meter (UV-meter model 5.0 digital, USA), respectively. Temperature of the cooling water bath was controlled by cold water circulated through copper coil. A magnetic stirring bar was used to facilitate the cooling. The mixture containing atrazine solution and catalyst in the beaker was stirred by an electric agitator with paddles.

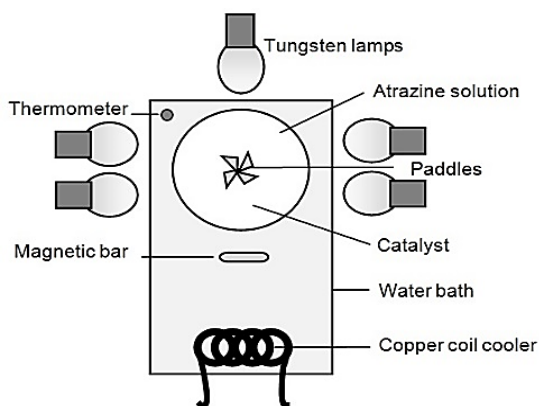


Fig. 2. Top view diagram of a batch reactor

2.4. Photocatalysis of atrazine

Firstly, an atrazine solution with a concentration 5.0 mg/L solution was prepared by dissolving atrazine (Fluka Analytical, 97.2%) in deionized water. The solution pH was 4.7-5.6. Then, 100 mL of atrazine solution and 0.1 g of catalyst powder were introduced to the beaker in the reactor. The mixture was stirred for 60 min to allow a saturated adsorption. Then, the tungsten lamps were switched on. A 1-mL sample was collected periodically using a syringe and PTFE syringe filter (diameter = $0.45 \mu\text{m}$) to separate the solution from the suspended catalyst powder. The experiments were performed in triplicate. The catalyst with the best performance was further studied to understand the reaction kinetics using $0.9\text{-}9.5 \text{ mg/L}$ of atrazine initial concentration. In addition, the effect of natural organic matter using 50.0 mg/L of humic acid (Sigma Aldrich Chemistry) on the decomposition of atrazine was investigated.

2.5. Analysis of atrazine

The concentration of atrazine was determined by high performance liquid chromatography (HPLC, Agilent Technologies) equipped with Hypersil C18 ODS ($4.0 \times 125 \text{ mm}$, $5 \mu\text{m}$) column and diode-array detector (HPLC-DAD 1200 series). The HPLC conditions for the atrazine analysis were similar to the report by Fu (2009). The UV detector was set at 254 nm . The mobile phase consisted of 55% of methanol (RCI Labscan Limited, HPLC grade, 99.99%) and 45% of deionized water with a flow rate of 1.0 mL/min . The methanol and deionized water were filtered and degassed for 60 min before loading to the HPLC. A column temperature was 40°C and injection

volume was $80 \mu\text{L}$. Total organic carbon (TOC) was determined by a TOC Analyzer (Shimadzu TOC-V CPH) with an autosampler (Shimadzu ASI-V) based on CO_2 quantification from high temperature catalytic combustion by a non-dispersive IR detector. The injection volume was $50 \mu\text{L}$ and the retention time was 2 min .

The intermediates produced during the photocatalytic degradation of atrazine was analyzed by a liquid chromatograph coupled with a mass spectrometer (LC-MS, Waters 3100 mass detector equipped with Waters 2695 separation module). The samples were infused into the mass spectrometer at a flow rate of 0.4 mL/min with an injection volume of $5.00 \mu\text{L}$. The heated capillary temperature was 120°C , and the spray voltage was set to 3.7 kV . The electrospray was in the positive mode. The chromatographic conditions were the same as that of by HPLC.

2.6. Langmuir-Hinshelwood-Hougen and Watson (LHHW) kinetics

LHHW kinetics (Eq. 1) covers the adsorption property of pollutant on the catalyst surface coupled with the reaction occurring at the solid-liquid interface in photocatalytic process. k_r and K_{ads} was calculated based on the linear form (Eq. 2).

$$r_0 = (k_r K_{ads} C_0) / (1 + K_{ads} C_0) \quad (1)$$

where: k_r = reaction rate constant ($\text{mg/L}\cdot\text{min}$); K_{ads} = adsorption equilibrium constant (L/mg); C_0 = initial equilibrium concentration of atrazine (mg/L).

$$1/r_0 = (1/k_r K_{ads} C_0) + (1/k_r) \quad (2)$$

Initial photocatalytic degradation rate (r_0) was estimated using the three-point differentiation formula (Eq. 3) (Fogler, 2006). The r_0 calculation concerns only the experimental data obtained during the first minute of irradiation time to minimize variation from the competitive effect of intermediates, pH changes, and other parameters.

$$r_0 = (-3C_0 + 4C_1 - C_2) / 2\Delta t \quad (3)$$

where; C = concentration of atrazine at reaction time t (mg/L); $\Delta t = t_2 - t_1$ (min)

3. Results and discussion

3.1. Characteristics of 0.005Ag-0.005Ce-ZnO, 0.005Fe-0.005Ce-ZnO, and 0.005Cu-0.005Ce-ZnO

XRD patterns of 0.005Ag-0.005Ce-ZnO, 0.005Fe-0.005Ce-ZnO, 0.005Cu-0.005Ce-ZnO, and ZnO are shown in Fig. 3(a). The diffraction peaks from all catalysts consisted characteristic peaks of ZnO in wurtzite structure (JCPDS, 36-1451). Sharp peaks indicated high crystallinity and their crystalline sizes calculated using Debye-Scherrer equation were similar (Table 1).

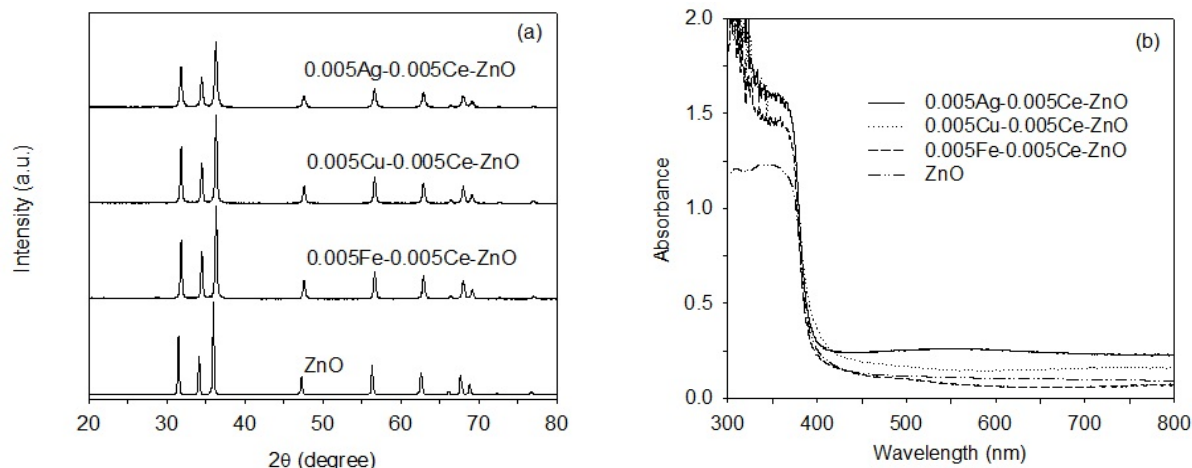


Fig. 3. (a) XRD patterns and (b) UV-vis-DRS spectra of catalyst synthesized using sticky rice starch as template in comparison with ZnO

The peak corresponding to Ag, Fe, Cu, and Ce dopants were not observed likely due to the low loading. UV-Vis-DRS spectra of 0.005Ag-0.005Ce-ZnO, 0.005Fe-0.005Ce-ZnO, 0.005Cu-0.005Ce-ZnO, and ZnO are shown in Fig. 3(b). The absorption of ZnO occurred mainly in the UV range. When doped with Ce, Ag, Cu, and Fe, the absorption in the UV range increased. The absorption in the visible range also increased in 0.005Ag-0.005Ce-ZnO and 0.005Cu-0.005Ce-ZnO. The result was consistent with a report by Tian et al. (2010) and Xin et al. (2008) that the absorption in the visible range by ZnO was increased after doping with Ag and TiO₂ with Cu, respectively. The change could be the key to enhance photocatalytic activity under visible light irradiation.

Surface areas of 0.005Ag-0.005Ce-ZnO, 0.005Fe-0.005Ce-ZnO, 0.005Cu-0.005Ce-ZnO, and ZnO are reported in Table 1. All samples still had low surface area. Modification by template and doping resulted in a slight increase in the surface area.

Table 1. Surface areas and crystallite size of catalyst synthesized using sticky rice starch as template in comparison with ZnO

Catalyst	Surface area (m ² /g)	Crystallite size (nm)
0.005Ag-0.005Ce-ZnO	17	31.6
0.005Cu-0.005Ce-ZnO	23	37.5
0.005Fe-0.005Ce-ZnO	15	38.0
ZnO	7	65.0

3.2. Photocatalysis of atrazine

Fig. 4 shows relative concentrations of atrazine (C/C_0) in the dark and under visible light in the presence of ZnO with various dopants. With 0.005Cu-0.005Ce-ZnO, the atrazine removal was not observed either in the dark or under visible light probably due

to insufficient amount of Cu. According to a review by Kumar and Rao (2015), the amount of Cu loading to produce an active photocatalyst was between 0.5 and 2.0 wt% for the degradation of dyes. The atrazine removal under visible light was observed on 0.005Fe-0.005Ce-ZnO and 0.005Ag-0.005Ce-ZnO. The Ag-doped catalyst was more active probably from the higher absorption in the range of visible light (Pongwan et al., 2012). The activity may be from a synergistic effect between silver and Ce⁴⁺ to trap electron with its subsequent transfer to the adsorbed oxygen (Kumar and Rao, 2015). Since 0.005Ag-0.005Ce-ZnO showed the highest atrazine removal, it was selected as a prototype for further study.

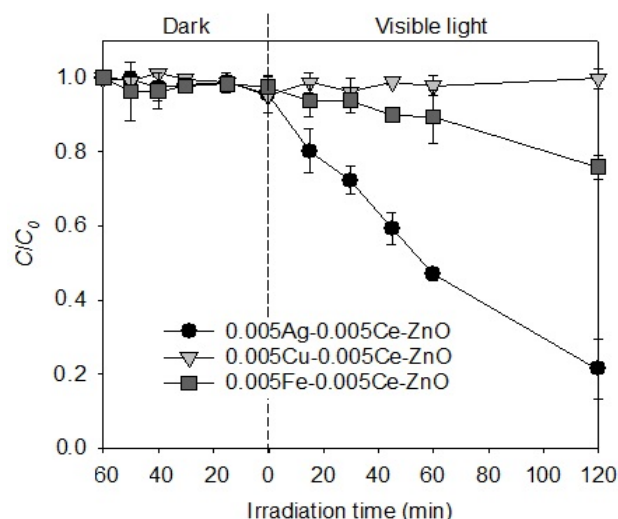


Fig. 4. Photocatalytic degradation of atrazine in the dark and under visible light on ZnO with various dopants

3.3. Langmuir-Hinshelwood-Hougen and Watson (LHHW) kinetics

Fig. 5(a) shows the decrease of atrazine from various initial concentrations during photocatalytic

degradation using 0.005Ag-0.005Ce-ZnO. According to the slope after irradiation, the faster degradation rate was observed in the sample with the higher initial concentration (see further discussion in Fig. 5c). Fig. 5b shows percent removal after 120 min. A higher percent removal was obtained from the solution with a lower concentration because the same amount of catalyst was used, producing a higher molar ratio of generated active radicals to atrazine molecules. Fig. 5c shows the initial degradation rates from different initial atrazine concentrations. The initial rates (r_0) increased with the initial concentration (C_0). The rates were low at the low concentration, then increased and became nearly plateau at high concentration. This behavior indicated the saturation-type Langmuir kinetics (Parra et al., 2004). With a higher initial concentration, there were more atrazine molecules

near the surface which could readily react with radicals such as $O_2\cdot$ and $\cdot OH$ generated by the irradiation. From the calculation of the linear LHHW equation ($R^2 = 0.9668$), the reaction rate constant (k_r) was 48.54 mg/L-min and equilibrium adsorption constant (K_{ads}) was 0.0060 L/mg. The k_r was approximately 10^4 -fold greater than the K_{ads} implying that the reaction occurred at the catalyst surface. These results agreed with the LHHW kinetics studies on photocatalytic degradation of atrazine (Parra et al., 2004; Lackhoff and Niessner, 2002). However, the K_{ads} values from this study and from the report by Lackhoff and Niessner (2002) were greater than the k_r explored by Parra et al. (2004). Such differences could be from various parameters such as atrazine concentration, catalyst type and loading, light source, pH, and temperature.

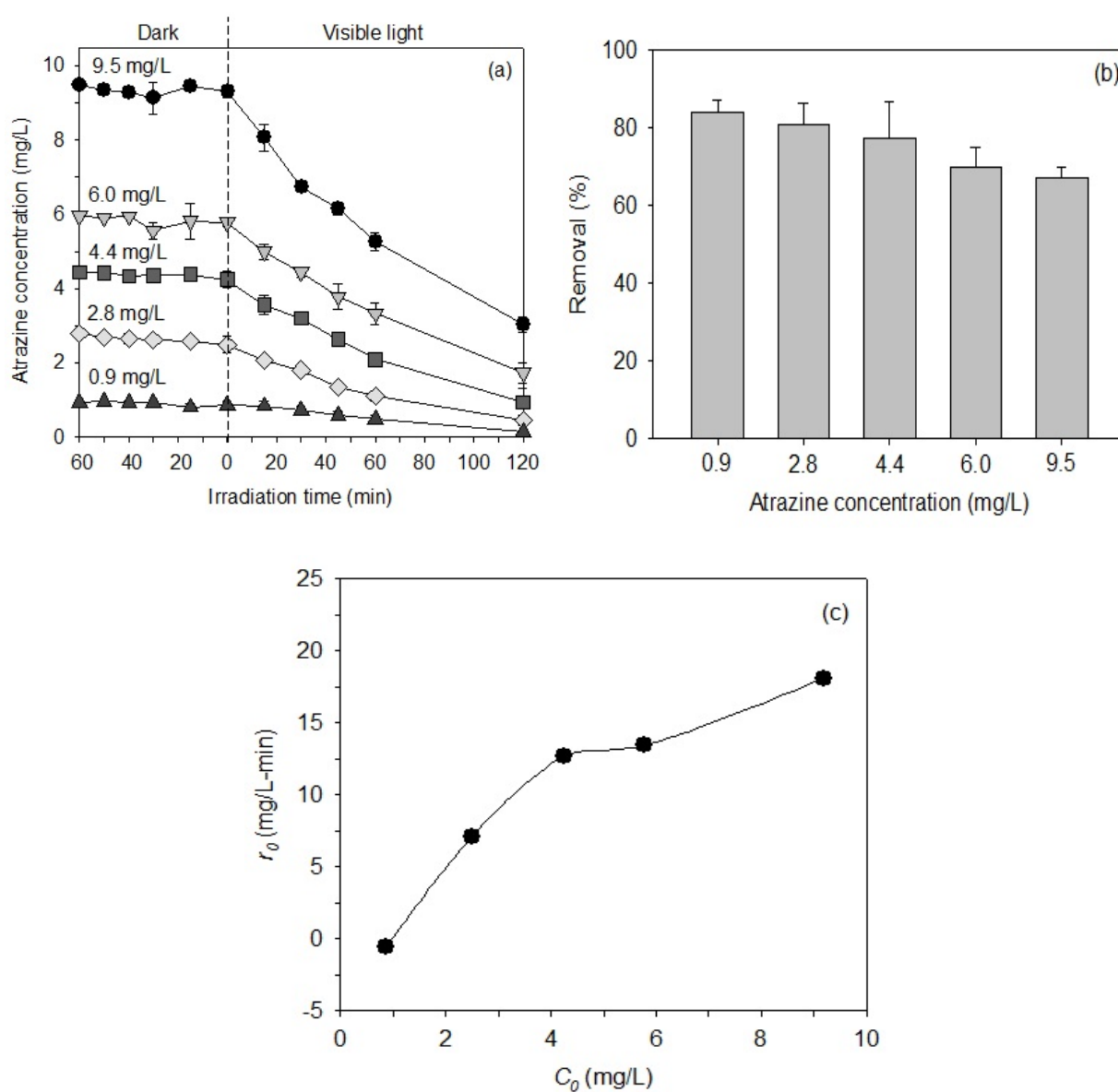


Fig. 5. (a) Photocatalytic degradation of atrazine by 0.005Ag-0.005Ce-ZnO with various initial concentration, (b) percent removal after 120 min of irradiation, and (c) initial rate of atrazine photocatalytic degradation as a function of atrazine initial concentration

3.4. Effect of natural organic matter

Atrazine is considered as a non-point source pollutant which always exists in nature with organic matters. Thus, this study was conducted using humic acid as a representative of natural organic matters. The atrazine removal by 0.005Ag-0.005Ce-ZnO in the presence and absence of humic acid is shown in Fig. 6. Lower degradation was observed in the presence of humic acid probably due to its ability to react with oxidative species (Liu et al., 2009). Chandran et al. (2014) reported that the degradation of methylene blue using ZnO nanoparticles decreased with an increase in concentration of humic acid. The presence of humic acid lowered the solution pH as well as the formation of hydroxyl radicals.

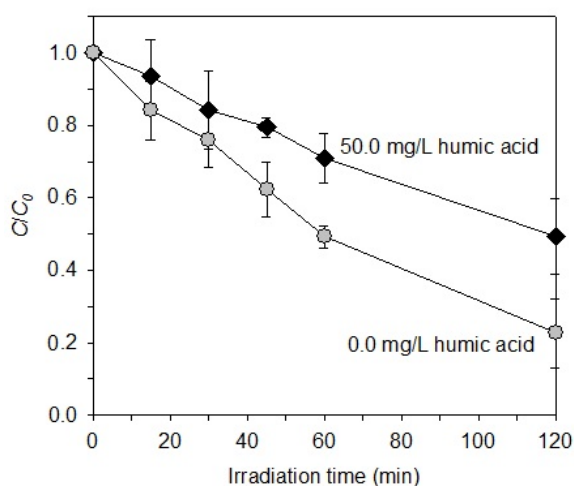


Fig. 6. Effect of natural organic matter on atrazine photocatalytic degradation using 0.005Ag-0.005Ce-ZnO

3.5. Evaluation of photocatalytic degradation pathway of atrazine

Fig. 7 presents the relative concentration of atrazine (C/C_0) and relative total organic compound (TOC/TOC_0) during the photocatalytic degradation using 0.005Ag-0.005Ce-ZnO. The degradation involved oxidation of lateral alkyl chains in the atrazine structure (Konstantinou and Albanis, 2002) leading to a large decrease of atrazine concentration. The observation of TOC suggests that atrazine changed to stable products. At 180 min of irradiation time, nearly 90% of atrazine was removed while the TOC was 64%. A similar observation of the TOC was reported from atrazine photocatalytic degradation using TiO_2 in supercritical water or hydrothermal water (Horikoshi and Hidaka, 2003).

The 60% decrease of TOC was consistent with the degradation of lateral alkyl chains in atrazine structure from eight carbons to three carbons as described by Eq. (4) in the literature (McMurray et al., 2006). The three carbon atoms in the final product are likely part of the triazine ring in cyanuric acid. In other studies, decomposition to cyanuric acid was seldom

reached in the catalytic decomposition (Huster et al., 1991; Minero et al., 1996; Pelizzetti et al., 1990) because the potential of photocatalytic degradation was inadequate. Under UV irradiation, atrazine photodegradation in the presence of fluoride ions or sodium persulfate proceeded through several steps which finally yielded cyanuric acid (Minero et al., 1996; Oh and Jenks, 2004).

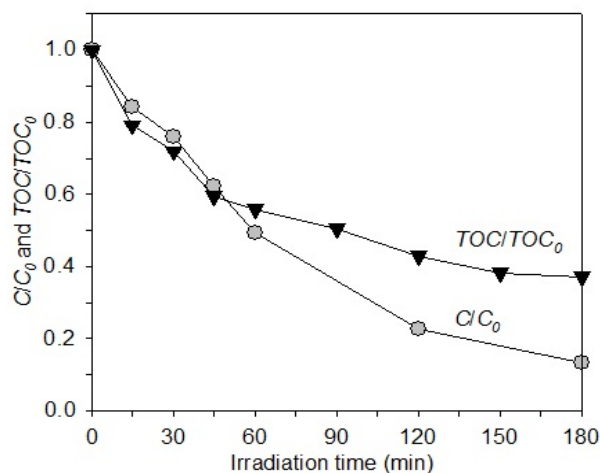
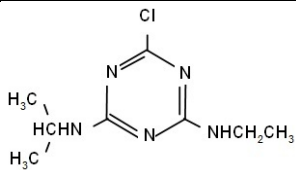
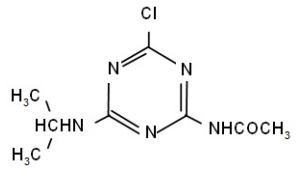
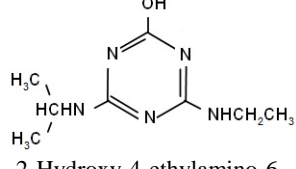
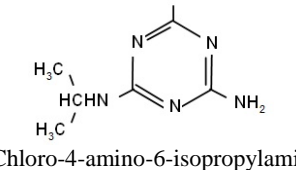
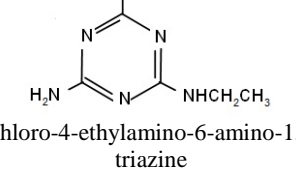
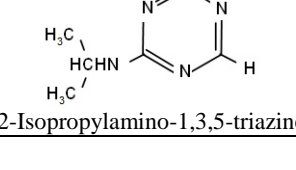


Fig. 7. Decrease of atrazine concentration (C) and total organic carbon (TOC) as a function of irradiation time on atrazine photocatalytic degradation using 0.005Ag-0.005Ce-ZnO

According to the reaction pathway of atrazine photocatalytic degradation studied by Lackhoff and Niessner (2002) and Minero et al. (1996), only five intermediates were found in this study using 0.005Ag-0.005Ce-ZnO under visible light irradiation (Table 2). Atrazine was transformed to those intermediates through lateral alkyl chain oxidation and dechlorination. The degradation seemed to end after 180 min but did not convert to the stable final product, cyanuric acid. This verification was consistent with the TOC results which reached 60% without triazine ring mineralization. The 3/8 TOC limit was unable to progress to the other steps with this catalyst (Carlin et al., 1990). Among the five intermediates, 2-isopropylamino-1,3,5-triazine (compound 5) has not been previously reported (Héquet et al., 2001; McMurray et al., 2006).

In general, organic compounds could be degraded by a photocatalytic reaction and finally mineralized to CO_2 and inorganic ions. However, the degradation could be retarded by the presence of cyanuric acid due to its resistance to photocatalytic conditions (Minero et al., 1997). Although cyanuric acid is nearly nontoxic and biodegradable, it could be considered as an inhibitor of photocatalytic processes in water purification, especially, when the water is contaminated by compounds containing 1,3,5-triazine ring in the structure.

Table 2. LC-MS identification of intermediates from atrazine photocatalytic degradation at 120 min of irradiation

Compound number	Compound structure and name	Molecular weight	m/z	Retention time (min)	Intensity
Atrazine	 2-Chloro-4-ethylamino-6-isopropylamino-1,3,5-triazine	215.5	216	3.419	3.7×10^7
1	 2-Chloro-4-acetamido-6-isopropylamino-1,3,5-triazine	229.5	229	0.879	4.1×10^6
2	 2-Hydroxy-4-ethylamino-6-isopropylamino-1,3,5-triazine	197.0	197	1.547	4.6×10^6
3	 2-Chloro-4-amino-6-isopropylamino-1,3,5-triazine	187.5	188	1.547	$\approx 3.9 \times 10^6$
4	 2-Chloro-4-ethylamino-6-amino-1,3,5-triazine	173.0	174	- (Found at 180 min of irradiation)	-
5	 2-Isopropylamino-1,3,5-triazine	138.0	137	1.547	$\approx 3.7 \times 10^6$

4. Conclusions

Zinc oxide (ZnO) was modified with sticky rice starch template and doped with Ce, Ag, Fe, and Cu (with molar ratio M/Ce/Zn of 0.005/0.005/1) and used for photodegradation of atrazine. The 0.005Ag-0.005Ce-ZnO showed the highest removal of atrazine in 180 min due to its greater absorbance in visible light range from UV-vis-DRS. The reaction behavior could be explained by Langmuir-Hinshelwood-Hougen and Watson (LHHW) kinetics. The k_r (48.54 mg/L-min) was much higher than K_{ads} (0.0060 L/mg) implying

that the photocatalytic reaction played an important role in the atrazine removal. The photodegradation was retarded by the presence of humic acid. TOC decrease of atrazine photocatalytic degradation reached 64%. Five intermediates were detected by LC-MS and 2-isopropylamino-1,3,5-triazine (compound 5) has not been previously reported.

Acknowledgements

This work was supported by Suranaree University of Technology, the Higher Education Research Promotion and National Research University Project of Thailand, Office of the Higher Education Commission.

References

- ARO, (2012), Agricultural Regulatory Office, Top 10 imported hazardous chemicals year 2012, Department of Agriculture, Ministry of Agriculture and Cooperative, Thailand, On line at: www.doa.go.th/ard/FileUpload/StatisticsHazardTop%2010%2055.pdf.
- Carlin V., Minero C., Pelizzetti E., (1990), Effect of chlorine on photocatalytic degradation of organic contaminants, *Environmental Technology*, **11**, 919-926.
- Chandran P., Netha S., Khanet S., (2014), Effect of humic acid on photocatalytic activity of ZnO nanoparticles, *Journal of Photochemistry and Photobiology B: Biology* **138**, 155-159.
- Chang C.J., Lin C.Y., Hsu M.H., (2014), Enhanced photocatalytic activity of Ce-doped ZnO nanorods under UV and visible light, *Journal of the Taiwan Institute of Chemical Engineers*, **45**, 1954-1963.
- Flynn K., Spellman T., (2009), Environmental levels of atrazine decrease spatial aggregation in the freshwater mussel, *Elliptio complanate*, *Ecotoxicology and Environment Safety*, **72**, 1228-1233.
- Fogler H.S., (2006), *Elements of Chemical Reaction Engineering*, 4th Edition, Pearson Publishing, United States of America.
- Hayes T., Haston K., Tsui M., Hoang A., Haeffele C., Vonk A., (2003), Atrazine-induced hermaphroditism at 0.1 ppb in American Leopard Frogs (*Rana pipiens*): laboratory and field evidence, *Environment Health Perspectives*, **111**, 568-575.
- Héquet V., Gonzalez C., Le Cloirec, P., (2001), Photochemical processes for atrazine degradation: methodological approach, *Water Research*, **35**, 4253-4260.
- Horikoshi S., Hidaka H., (2003), Non-degradable triazine substrate of atrazine and cyanuric acid hydrothermally and in supercritical water under the UV-illuminated photocatalytic cooperation, *Chemosphere*, **51**, 139-142.
- Hsu M.H., Chang C.J., (2014), Ag-doped ZnO nanorods coated metal wire meshes as hierarchical photocatalysts with high visible-light driven photoactivity and photostability, *Journal of Hazardous Materials*, **278**, 444-453.
- Hustert K., Moza P.N., Pouyet B., (1991), Photocatalytic degradation of s-triazine herbicides, *Toxicological and Environmental Chemistry*, **31**, 97-102.
- Jafari A.J., Dehghanifard E., Kalantary R.R., Gholami M., Esrafil A., Yari A.R., Baneshi M.M., (2016), Photocatalytic degradation of aniline in aqueous solution using ZnO nanoparticles, *Environmental Engineering and Management Journal*, **15**, 53-60.
- Khamdahsag P., Pattanasiriwisawa W., Nanny M.A., Gridanurak N., (2012), Comparative study of sticky rice starch and polyvinylpyrrolidone as templates for ZnO and Ce-ZnO synthesis, *Environmental Engineering and Management Journal*, **11**, 759-766.
- Konstantinou I.K., Albanis T.A., (2002), Photocatalytic transformation of pesticides in aqueous titanium dioxide suspensions using artificial and solar light: intermediates and degradation pathways, *Applied Catalysis B: Environmental*, **1310**, 1-17.
- Kruawal K., Sacher F., Werner A., Muller J., Knepper T.P., (2005), Chemical water quality in Thailand and its impacts on the drinking water production in Thailand, *Science of the Total Environment*, **340**, 57-70.
- Kumar S.G., Rao K.S.R.K., (2015), Zinc oxide based photocatalysis: tailoring surface bulk structure and related interfacial charge carrier dynamics for better environmental applications, *RSC Advances*, **5**, 3306-3342.
- Lackhoff M., Niessner R., (2002), Photocatalytic atrazine degradation by synthetic minerals, atmospheric aerosols, and soil particles, *Environmental Science and Technology*, **36**, 5342-5347.
- Li D., Haneda H., (2003), Photocatalysis of sprayed nitrogen-containing Fe₂O₃-ZnO and WO₃-ZnO composite powders in gas-phase acetaldehyde decomposition, *Journal of Photochemistry and Photobiology A: Chemistry*, **160**, 203-212.
- Li D., Haneda H., Ohashi N., Hishita S., Yoshikawa Y., (2004), Synthesis of nanosized nitrogen-containing MO_x-ZnO (M = W, V, Fe) composite powders by spray pyrolysis and their visible-light-driven photocatalysis in gas-phase acetaldehyde decomposition, *Catalysis Today*, **93-95**, 895-901.
- Liu C., Chen W., Sheng Y., Li L., (2009), Atrazine degradation in solar irradiation/ S-doped titanium dioxide treatment, On line at: http://ieeexplore.ieee.org/xpls/abs_all.jsp?arnumber=516-2423&tag=1.
- McMurray T.A., Dunlop P.S.M., Byrne J.A., (2006), The photocatalytic degradation of atrazine on nanoparticulate TiO₂ films, *Journal of Photochemistry and Photobiology A: Chemistry*, **182**, 43-51.
- Minero C., Maurino V., Pelizzetti E., (1997), Heterogeneous photocatalytic transformations of s-triazine derivatives, *Research on Chemical Intermediates*, **23**, 291-310.
- Minero C., Pelizzetti E., Malato S., Blanco J., (1996), Large solar plant photocatalytic water decontamination: degradation of atrazine, *Solar Energy*, **56**, 411-419.
- Oh Y.C., Jenks W.S., (2004), Photocatalytic degradation of a cyanuric acid, a recalcitrant species, *Journal of Photochemistry and Photobiology A: Chemistry*, **162**, 323-328.
- Parra S., Stanca S.E., Guasaquillo I., Thampi K.R., (2004), Photocatalytic degradation of atrazine using suspended and supported TiO₂, *Applied Catalysis B: Environmental*, **51**, 107-116.
- Pelizzetti E., Maurino V., Minero C., Carlin V., Pramauro E., Zerbini O., Tosato M.L., (1990), Photocatalytic Degradation of Atrazine and Other s-Triazine Herbicides, *Environmental Science and Technology*, **24**, 1559-1565.
- Pongwan P., Inceesungvorn B., Wetchakun K., Phanichphant S., Wetchakun N., (2012), Highly efficient visible-light-induced photocatalytic activity of Fe-doped TiO₂ nanoparticles, *Engineering Journal*, **16**, 143-151.
- Ren C., Yang B., Wu M., Xu J., Fu Z., Iv Y., Guo T., Zhao Y., Zhu C., (2010), Synthesis of Ag/ZnO nanorods array with enhanced photocatalytic performance, *Journal of Hazardous Materials*, **182**, 123-129.
- Sukjaroen K., Prayoonrat P., (2001), Effect of certain herbicides on Mungbean, On line at: <http://plantpro.doae.go.th/weed-research/P-44.pdf>.
- Tian C., Li W., Pan K., Zhang Q., Tian G., Zhou W., Fu H., (2010), One pot synthesis of Ag nanoparticle modified ZnO microspheres in ethylene glycol medium and their enhanced photocatalytic performance, *Journal of Solid State Chemistry*, **183**, 2720-2725.
- U.S. EPA., (1988), Atrazine - dietary exposure and oncogenic risk assessment, Office of Pesticides and Toxic Substances, U.S. Environmental Protection Agency, Washington, D.C., On line at: <https://archive.epa.gov/pesticides/chemicalsearch/chemical/foia/web/pdf/080803/080803-101.pdf>

- U.S. EPA., (2003), Atrazine chemical summary, U.S. EPA, toxicity and exposure assessment for children's health, U.S. Environmental Protection Agency, Washington, D.C., On line at: https://archive.epa.gov/region5/teach/web/pdf/atrazine_summary.pdf
- Vidyasagar C.C., Arthoba Naik Y., Venkatesh T.G., Viswanatha R., (2011), Solid-state synthesis and effect of temperature on optical properties of Cu-ZnO, Cu-CdO, and CuO nanoparticles, *Powder Technology*, **214**, 337-343.
- WQMB, (2012), Water Quality Management Bureau, Criterion, regulation, and standard related to water pollutant from agriculture, Pollution Control Department, Ministry of Industry, Thailand, On line at: <http://wqm.pcd.go.th/water/images/stories/agriculture/manual/2555/181055.pdf>.
- Xin B., Wang P., Ding D., Liu J., Ren Z., Fu H., (2008), Effect of surface species on Cu-TiO₂ photocatalytic activity, *Applied Surface Science*, **254**, 2569-2574.
- Yola M.L., Eren T., Atar N., (2014), A novel efficient photocatalyst based on TiO₂ nanoparticles involved boron enrichment waste for photocatalytic degradation of atrazine, *Chemical Engineering Journal*, **250**, 288-294.
- Zhang D., Liu X., Wang X., (2011), Growth and photocatalytic activity of ZnO nanosheets stabilized by Ag nanoparticles, *Journal of Alloys and Compounds*, **509**, 4972-4977.